Int. J. Electrochem. Sci., 15 **(2020)** 3969 – 3979, doi: 10.20964/2020.05.54

International Journal of
ELECTROCHEMICAL
SCIENCE
www.electrochemsci.org

Simultaneous Determination of Dopamine and Uric Acid on a MoS_2-CPtNPs Nanocomposite-Modified Electrode

Zhiqiang Zhu[1], *Chen Jin*[1], *Xiangyang Miao*[1], *Ye Shen*[2,*]

[1] Suzhou Chien-shiung Institute of Technology
[2] Suzhou Institute of Nano-Tech and Nano-Bionics
[*]E-mail: yshen2010@sinano.ac.cn

Received: 8 January 2020 / *Accepted:* 18 February 2020 / *Published:* 10 April 2020

Clover-like platinum nanoparticle-supported MoS_2 (MoS_2-CPtNPs) nanocomposites were employed to construct an electrochemical sensor for the simultaneous determination of dopamine (DA) and uric acid (UA). The MoS_2-CPtNPs nanocomposite was synthesized by a microwave-assisted hydrothermal method, and it was characterized by TEM and XRD. Two well-defined oxidation peaks of DA and UA located at 0.096 V and 0.304 V (vs. SCE) were obtained with the MoS_2-CPtNPs nanocomposite-modified electrode. A sufficient peak separation (208 mV) and a large peak current allowed the simultaneous determination of DA and UA by differential pulse voltammetry (DPV) with this modified electrode. Under optimal conditions, the MoS_2-CPtNPs-modified electrode could determine DA and UA down to 0.39 μM and 1.8 μM, respectively, with high selectivity. Moreover, an accepted relative standard deviation (RSD) and good recovery in serum were established. The above results suggest that the MoS_2-CPtNPs nanocomposite has potential applications in analytical and diagnostic research.

Keywords: electrochemistry; dopamine; simultaneous determinations

1. INTRODUCTION

The concentrations of dopamine (DA) and uric acid (UA) are greatly related to metabolism and diseases. For example, DA plays an important role in the functioning of kidneys and hormones, and in the cardiovascular system and central nervous system. Moreover, abnormal levels of DA are related to drug addiction and Parkinson's disease [1-4]. UA is the metabolism product of purine, which is a biomarker for monitoring hyperuricaemia and gout [5, 6].

Electrochemical techniques exhibit superior advantages in biological molecule analysis, disease diagnosis and homeland security, due to their fast response, high sensitivity, simple operation and low cost. Because DA and UA often coexist in human serum, it is difficult to efficiently distinguish them

with solid electrodes. Therefore, the development of modified electrodes for the simultaneous determination of DA and UA has become a popular method [7-9]. Compared with organic molecules, inorganic materials, especially nanomaterials such as carbon nanotubes, silicon nanowires, noble metal nanoparticles, metal oxides, graphene and its derivatives, have been extensively used to construct modified electrodes for DA and UA detection due to their excellent chemical and physical properties [10-14].

Two-dimensional molybdenum disulfide (MoS_2) is a graphene-like layered nanomaterial that has received increasing interest in electrochemical sensors because of its unique structure and electrical properties [15-19]. In this study, MoS_2 is used as a substrate to load platinum nanoparticles. Clover-like platinum nanoparticles (CPtNPs) are grown in situ on the surface of MoS_2 nanosheets via a microwave-assisted hydrothermal synthesis. The as-prepared MoS_2-CPtNPs nanocomposites exhibit excellent electrocatalytic activity towards DA and UA, and can efficiently distinguish DA and UA with sufficient peak separation. Furthermore, the large peak current demonstrates that this MoS_2-CPtNPs nanocomposite-modified electrode determines DA and UA with high selectivity. Experimental data show that the modified electrode can individually or simultaneously determine DA and UA in a buffer and in real samples with satisfactory results, suggesting that the designed MoS_2-CPtNPs nanocomposites possess great potential application in the construction of electrochemical sensors for chemical/biological molecule detection.

2. EXPERIMENTAL

2.1. Chemicals and reagents

Potassium platinochloride (K_2PtCl_4), N,N-dimethylformamide (DMF) and potassium iodide (KI) were purchased from Sinopharm Chemical Reagent Co., Ltd (Shanghai, China). Polyvinylpyrrolidone (PVP) and molybdenum (IV) sulfide (MoS_2, <2 mm, 99%) were purchased from Sigma-Aldrich Ltd. Other chemicals were analytical grade and used without further purification. All aqueous solutions were prepared with twice-deionized water.

2.2. Apparatus

All electrochemical measurements were tested on a CHI660E electrochemical workstation (Shanghai Chenhua Co., China) with a conventional three-electrode system. Different modified glassy carbon electrodes (GCEs), a saturated calomel electrode (SCE) and a platinum wire electrode were used as the working electrode, the reference electrode and the counter electrode, respectively. Electrolyte solutions were deoxygenated with nitrogen bubbling for at least 30 min, and a nitrogen atmosphere was kept over the solution during the electrochemical measurements.

Transmission electron microscopy (TEM) images were taken on a Hitachi H-7500 electron microscope (120 kV). Powder X-ray diffraction (XRD) was performed on a D/max-γB diffractometer.

2.3. Preparation of MoS_2 nanosheets

Single-layer MoS_2 nanosheets were prepared according to published works with some modifications [20-22]. In an argon atmosphere, n-butyllithium hexane solution was added to MoS_2 powder in a 2:1 mole ratio and then stirred well. After sonication for 180 min, the mixture was left for 30 min. The excess n-butyllithium was removed, and the lithium-intercalated MoS_2 was exfoliated by adding Ar-saturated H_2O. The MoS_2 nanosheets were collected by centrifugation at 12000 rpm three times.

2.3. Synthesis of MoS_2-CPtNPs nanocomposites and Pt nanoparticles

MoS_2-CPtNPs nanocomposites were synthesized according to the literature with some modifications [23, 24]. Briefly, 0.1 g KI and 0.25 g PVP were added into 240 μL (100 mM) potassium platinochloride (K_2PtCl_4) solution and stirred well for 30 min. Two millimolar DMF and a MoS_2 nanosheet suspension were mixed and stirred well for 30 min. The above two mixtures were transferred to a 20-mL erlenmeyer flask and then magnetically stirred for 15 min. The mixed solution was heated in a microwave reactor at 130°C for 30 min. Subsequently, the MoS_2-CPtNPs nanocomposites were centrifuged and washed twice at room temperature. Then, the final products were stored at 4°C for further use. For comparison, Pt nanoparticles were synthesized by a similar method [25] and characterized by TEM.

2.4. Preparation of the modified electrode

All electrodes were polished with 0.3 μm and 0.05 μm alumina. Then, the electrodes were sonicated in ethanol and deionized water in sequence. After cleaning, MoS_2-CPtNPs nanocomposites were dropped onto a glassy carbon electrode surface to form a MoS_2-CPtNPs nanocomposite-modified electrode, which was defined as MoS_2-CPtNPs/GCE. MoS_2/GCE and PtNPs/GCE were prepared by the same modification process.

3. RESULTS AND DISCUSSION

3.1. Characterization of the MoS_2-CPtNPs nanocomposites and PtNPs

The morphologies of the MoS_2-CPtNPs nanocomposites and Pt nanoparticles (PtNPs) were characterized by TEM (Fig. 1). With the addition of K_2PtCl_4, clover-like Pt nanoparticles (CPtNPs) grew in situ on the surface of the MoS_2 nanosheets (Fig. 1A). As shown in Fig. 1B, the diameter of CPtNPs on the MoS_2 surface was approximately 15.3±2.0 nm, which was smaller than that of pure PtNPs (16.2±2.2 nm, Fig. 1C and 1D). The shape of the PtNPs was similar to that supported on the MoS_2 nanosheets. XRD was used to further prove the successful synthesis of MoS_2-CPtNPs nanocomposites. As shown in Fig. S1, the X-ray diffractions at 39.62°, 46.10° and 67.22° were

assigned to the Pt(111), (200) and (220) planes (JCPDS 04-0802), respectively, which was consistent with the literature [24].

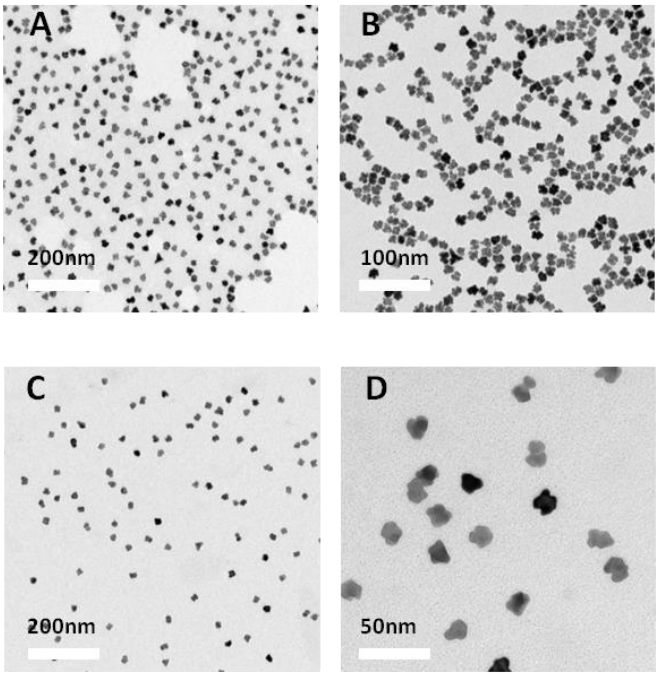

Figure 1. TEM images of the (A, B) MoS_2-CPtNPs nanocomposites and (C, D) Pt nanoparticles.

3.2. Electrochemical behaviours of MoS_2-CPtNPs nanocomposites

The electrochemical properties of the MoS_2-CPtNPs nanocomposites were investigated by electrochemical measurements. In accordance with previous reports [26, 27], no obvious peaks were observed with MoS_2/GCE (Fig. S2), and typical electrochemical behaviour of Pt was obtained with PtNPs/GCE and MoS_2-CPtNPs/GCE in a 0.1 M H_2SO_4 solution, indicating that MoS_2-CPtNPs nanocomposites and PtNPs had been prepared. The electron transfer of modified electrodes was investigated by electrochemical impedance spectroscopy (EIS). As shown in Fig. 2A, the electron transfer resistance (R_{et}) of MoS_2/GCE was larger than that of bare GCE, which was ascribed to the poor conductivity of the MoS_2 nanosheet [28]. After decorating with CPtNPs, a low R_{et} was recorded with MoS_2-CPtNPs/GCE (208.2 Ω vs. 527.1 Ω), suggesting that the electron conductivity was improved by the functionalization of CPtNPs on the MoS_2 sheet, which was similar to that of a previous reference [16].

The feasibility of the electrochemical detection of DA and UA with MoS_2-CPtNPs/GCE was then tested by cyclic voltammetry (CV, Fig. S3) and differential pulse voltammetry (DPV) measurements The results indicated that MoS_2-CPtNPs/GCE could efficiently determine DA and UA. Fig. 2B shows the DPV curves of PtNPs/GCE, MoS_2/GCE and MoS_2-CPtNPs/GCE for simultaneous determination of DA and UA. Two larger and well-defined oxidation peaks were observed at 0.096 V and 0.304 V (vs. SCE) with MoS_2-CPtNPs/GCE compared with that of PtNPs/GCE and MoS_2/GCE, respectively, indicating that the MoS_2-CPtNPs/GCE exhibited excellent electrocatalytic ability towards

DA and UA. All experimental results proved that the designed MoS_2-CPtNPs/GCE could be used to efficiently analyse DA and UA.

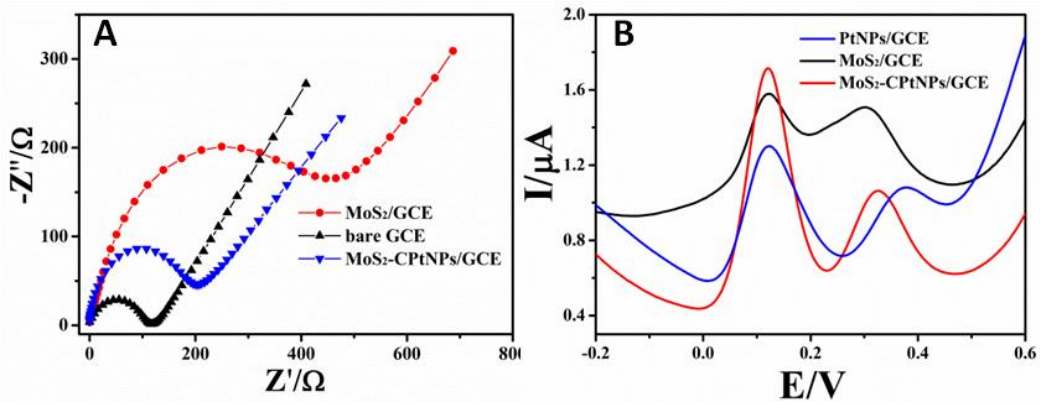

Figure 2. (A) Nyquist plots of MoS_2/GCE, MoS_2-CPtNPs/GCE and bare GCE. (B) DPV curves obtained with PtNPs/GCE, MoS_2/GCE and MoS_2-CPtNPs/GCE in 0.2 mM PB solution containing 40 μM DA and 50 μM UA.

3.3. Optimization of determination conditions

To obtain the best detection performance, the experimental conditions were optimized, including the concentration of the MoS_2-CPtNPs nanocomposites and the pH value of the detection buffer. From the results shown in Fig. 3A, two high and well-defined oxidation peaks of DA and UA were obtained when the MoS_2-CPtNPs nanocomposite was 5 μg/mL. A higher concentration of the MoS_2-CPtNPs nanocomposite did not result in a larger peak current. Therefore, a nanocomposite concentration of 5 μg/mL were employed in the following experiments.

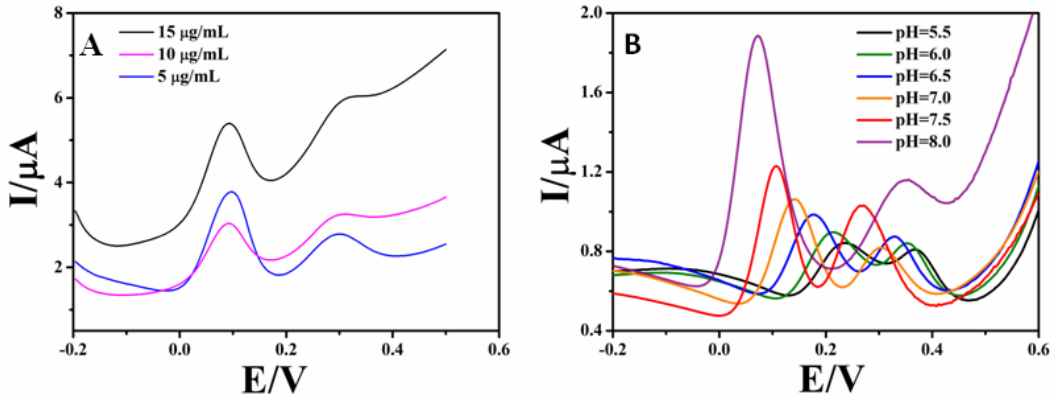

Figure 3. Effect of the (A) MoS_2-CPtNPs nanocomposite concentration and (B) pH value on the detection performance of DA and UA with MoS_2-CPtNPs/GCE.

The effect of the pH value on the detection performance was also investigated. As shown in Fig. 3B, the oxidation peaks shifted negatively with pH values ranging from 5.5 to 8.0. Low

background currents and well-defined oxidation peaks of DA and UA were obtained when the pH value was 7.5. Therefore, we chose pH=7.5 as the optimal detection condition.

3.4. Analysis performance of the different modified electrodes

The analysis performance of the different modified electrodes for the determination of DA without UA was first evaluated. As shown in Fig. 4A and Fig. 4C, both MoS_2/GCE and PtNPs/GCE exhibited good electrocatalytic ability towards DA. The peak currents of MoS_2/GCE and PtNPs/GCE increased with increasing concentrations of DA ranging from 3 μM-200 μM and 5 μM to 200 μM, respectively.

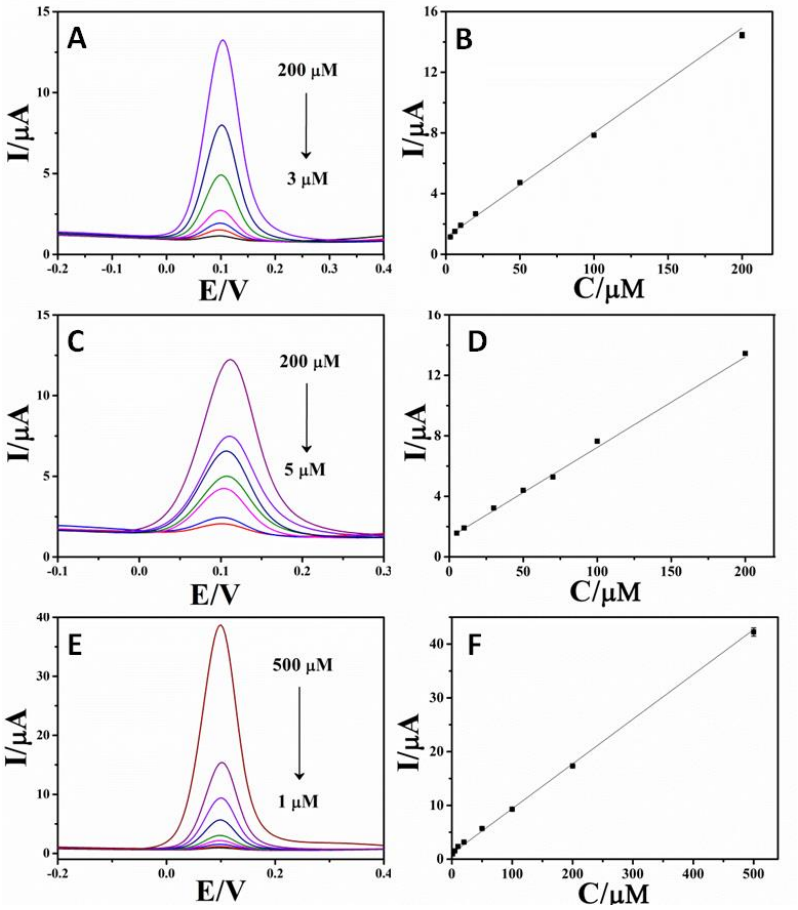

Figure 4. (A) DPV curves of different DA concentrations with MoS_2/GCE. (B) The relationship between peak current and DA concentration with MoS_2/GCE. (C) DPV curves of different DA concentrations with PtNPs/GCE. (D) The relationship between peak current and DA concentration with PtNPs/GCE. (E) DPV curves of different DA concentrations with MoS_2-CPtNPs/GCE. (F) The relationship between peak current and DA concentration with MoS_2-CPtNPs/GCE.

According to the linear range, the detection limit could be calculated as 0.18 μM with MoS_2/GCE (Fig. 4B) and 0.17 μM with PtNPs/GCE (Fig. 4D). Compared to the above electrodes, better detection performance was obtained with MoS_2-CPtNPs/GCE, including a wider linear range (1-

500 μM) and lower detection limit (0.12 μM). Interestingly, the peak current of DA at MoS_2-CPtNPs/GCE was larger than those of PtNPs/GCE and MoS_2/GCE, suggesting that MoS_2-CPtNPs nanocomposites possessed better electrocatalytic ability. This result was in agreement with the conclusion obtained from Fig. 2.

Selective determination of DA and UA with MoS_2-CPtNPs/GCE was also tested, which is shown in Fig. 5. Generally, we kept one species concentration fixed and varied another species concentration. Fig. 5A shows the DPV curves of the selective determination of DA by fixing the UA concentration at 50 μM. The peak current with MoS_2-CPtNPs/GCE increased with the addition of DA in a range from 1-500 μM with a detection limit of 0.11 μM (Fig. 5B). It was noted that the peak current of UA remained almost constant. A similar result was obtained with MoS_2-CPtNPs/GCE for the selective detection of UA ranging from 5-1000 μM (Fig. 5C and 5D). The detection limit of selective UA detection was calculated as 1.7 μM.

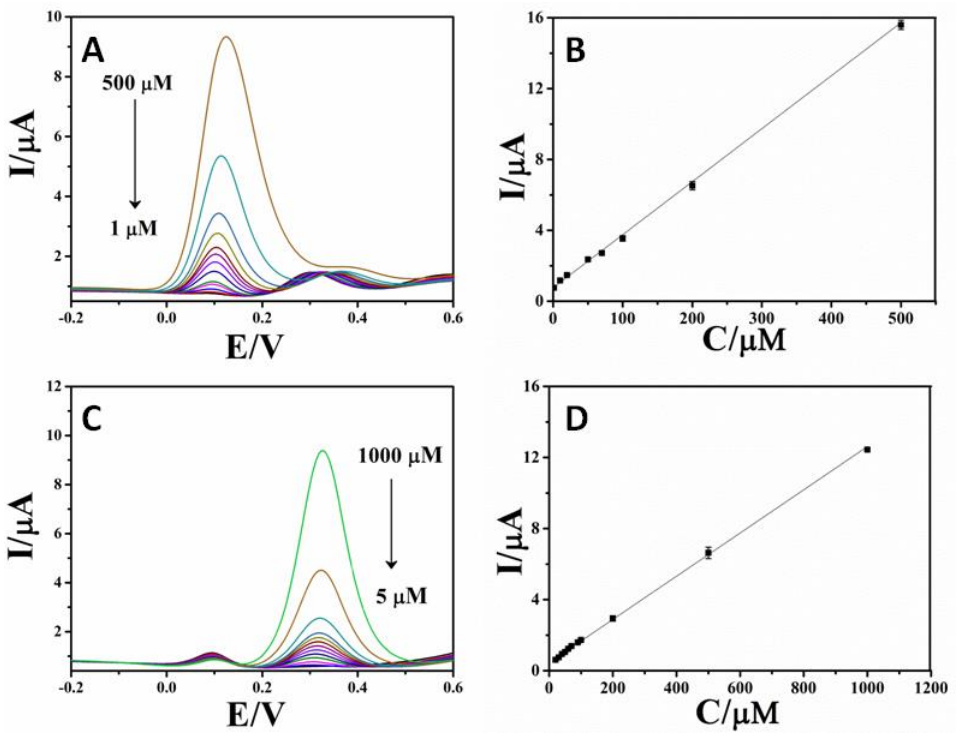

Figure 5. (A) DPV curves of MoS_2-CPtNPs/GCE for the selective determination of DA in a range of 1-500 μM. (B) The corresponding peak currents versus the DA concentration. (C) DPV curves of MoS_2-CPtNPs/GCE for the selective determination of UA in a range of 5-1000 μM. (D) The relationship between the peak currents and UA concentration.

On the basis of the above results, we tested the designed MoS_2-CPtNPs/GCE for the simultaneous detection of DA and UA. As shown in Fig. 6, the peak currents of DA and UA varied with increasing concentrations ranging from 5 μM-200 μM and 20-500 μM, respectively. As expected, the MoS_2-CPtNPs/GCE exhibited excellent electrocatalytic ability towards both DA and UA. Under the above condition, the detection limits of a simultaneous analysis of DA and UA were 0.39 μM and 1.8 μM, respectively. The difference in the detection limit of selective and simultaneous determination may be ascribed to the mutual influence of DA and UA. The analysis performances of MoS_2-

CPtNPs/GCE were comparable to or better than those of previously reported nanomaterial-modified electrodes (Table 1). Obviously, the MoS_2-CPtNPs/GCE showed wide linear ranges, a large peak separation, and low detection limits for the simultaneous detection of DA and UA.

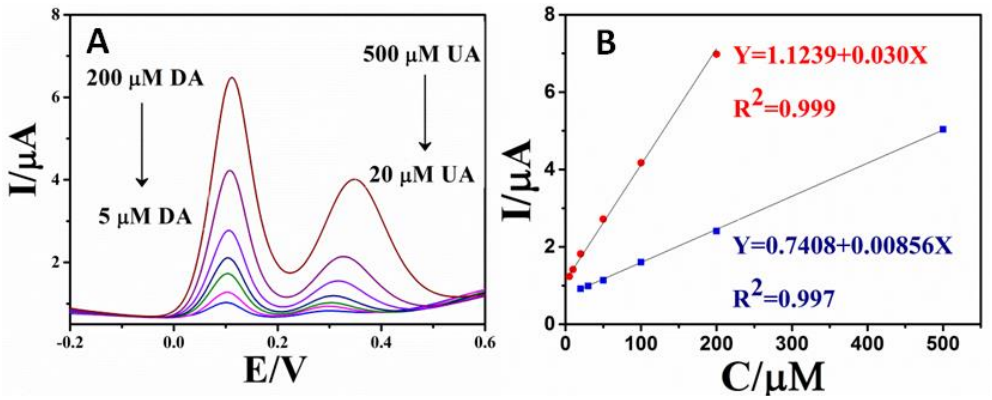

Figure 6. (A) DPV curve of MoS_2-CPtNPs/GCE for the simultaneous determination of DA and UA. (B) The corresponding peak current of DA (red) and UA (blue) versus the DA and UA concentration, respectively.

Table 1. Performance comparison of the simultaneous determination of DA and UA with sensors based on different matrices.

Electrode	DA–UA (mV)	Analyte	Linear range (μmol L^{-1})	Detection limit (μmol L^{-1})	References
Poly(4-aminobutyric acid)-modified GCE	136	DA	5.0-100.0	1.0	29
		UA	1.0-80.0	0.5	
Poly(Evans Blue)-modified GCE	180	DA	1-10	0.25	30
		UA	30-110	2.0	
PtNPs/RGO[a]-modified GCE	163	DA	10-170	0.25	31
		UA	10-130	0.45	
Au/RGO-modified GCE	110	DA	6.8-41	1.4	32
		UA	8.8-53	1.8	
RGO/carbon fibre electrode	163	DA	1.5-224.82	0.77	33
		UA	6-899.3	2.3	
PtAu hybrid film-modified electrodes	170	DA	24-384	24	34
		UA	21-336	21	
ERGO[b]-modified electrode	130	DA	0.5-60	0.5	35
		UA	0.5-60	0.5	
AgNPs/RGO[a]-modified electrode	124	DA	10-800	5.4	36
		UA	10-800	8.2	
AuCo NPs/HS-GR/GCE [c]	~120	DA	2.1-21.1	0.1	37
		UA	9-60	1	
MoS_2-CPtNPs-modified electrode	208	DA	1-500	0.11	this work
		UA	5-1000	1.7	

[a] reduced graphene oxide
[b] electrochemically reduced graphene oxide
[c] AuCo alloy nanoparticle/HS-graphene-modified electrode

3.5. Determination of DA and UA in serum

The potential application of the MoS_2-CPtNPs/GCE for the analysis of DA and UA in serum was investigated by using a standard addition method, which was performed in 1% human serum (pH 7.5). As listed in Table 2, an acceptable relative standard deviation (RSD, <5%) and recovery (98%-

102%) were obtained. These results proved that the prepared MoS_2-CPtNPs nanocomposite was an ideal nanomaterial to construct electrochemical sensors for the detection of chemical or biological molecules.

Table 2. Determination of DA and UA in serum samples (n=3).

Sample	Added (μM)		Recovery (%)		RSD (%)	
	DA	UA	DA	UA	DA	UA
1	5.00	20.0	99.2	98.5	0.9	3.1
2	10.0	30.0	98.8	100.9	2.6	1.2
3	20.0	50.0	101.8	101.5	4.5	2.5

4. CONCLUSIONS

In summary, we successfully fabricated clover-like PtNPs-decorated MoS_2 nanocomposites via a microwave-assisted synthesis method and used them to construct a modified electrode for the selective and simultaneous determination of DA and UA with high sensitivity. Under optimal conditions, MoS_2-CPtNPs/GCE exhibited excellent electrocatalytic ability towards DA and UA, which could simultaneously be determined as low as 0.39 μM DA and 1.8 μM UA, respectively. A real sample analysis further proved that the designed MoS_2-CPtNPs nanocomposites have great potential application in the construction of electrochemical sensors for target molecule detection.

ACKNOWLEDGEMENTS
This work was supported by the projects of the Enterprise Practice for Young Teachers in Jiangsu Province (No. 2018QYSJ097) and the Science and Technology Planning Project of Taicang (No. 2016YYJC07).

SUPPORTING MATERIAL:

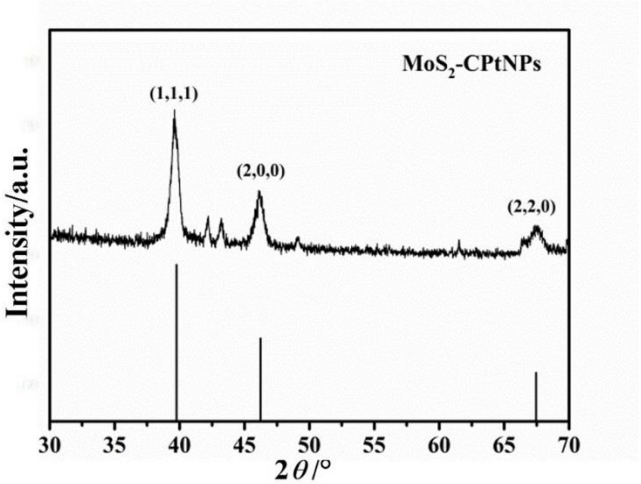

Figure S1. X-ray diffraction patterns of the MoS_2-CPtNPs nanocomposite.

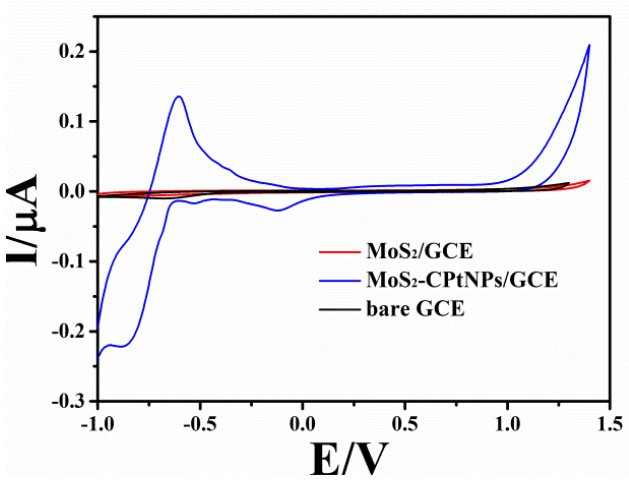

Figure S2. Cyclic voltammograms of MoS_2/GCE, MoS_2-CPtNPs/GCE and bare GCE.

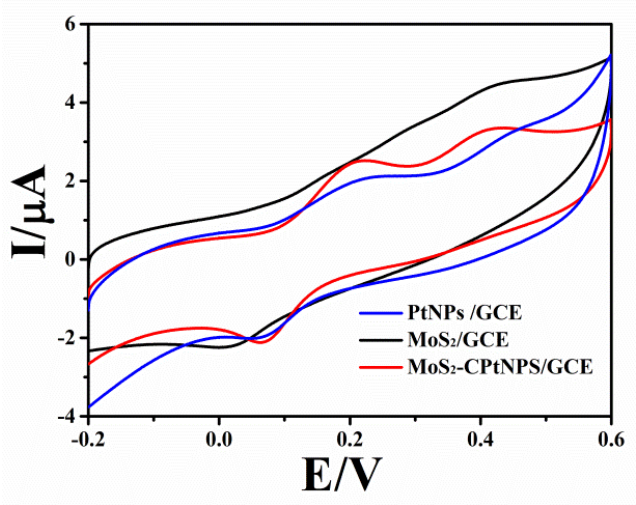

Figure S3. CV with PtNPs/GCE, MoS_2/GCE and MoS_2-CPtNPs/GCE in a N_2-saturated solution (0.2 mM PB) containing 40 μM DA and 50 μM UA.

References

1. J. W. Mo and B. Ogorevc, *Anal. Chem.*, 73 (2001) 1196.
2. N. G. Shang, P. Papakonstantinou, M. Mcmullan, M. Chu, A. Stamboulis, A. Potenza, S. S. Dhesi and H. Marchetto, *Adv. Funct. Mater.*, 18 (2010) 3506.
3. C. R. Raj, T. Okajima and T. Ohsaka, *J. Electroanal. Chem.*, 543 (2003) 127.
4. G. R. Ma, H. Xu, F. G. Xu, L. Wang, *Int. J. Electrochem. Sci.*, 12 (2017) 7365.
5. P. K. Aneesh, S. R. Nambiar, T. P. Rao and A. Ajayaghosh, *Anal. Methods*, 6 (2014) 5322.
6. W. Zhang, R. Yuan, Y. Q. Chai, Y. Zhang and S. H. Chen, *Sensor. Actuat. B-Chem*, 166 (2012) 601.
7. W. Zhang, Y. Chai, R. Yuan, S. Chen, J. Han and D. Yuan, *Anal. Chim. Acta*, 756 (2012) 7.
8. A. Babaei, M. Zendehdel, B. Khalilzadeh and A. Taheri, *Colloids Surf. B*, 66 (2008) 226.
9. N. Nontawong, M. Amatatongchai, W. Wuepchaiyaphum, S. Chairam, S. Pimmongkol, S. Panich, S. Tamuang and P. Jarujamrus, *Int. J. Electrochem. Sci.*, 13 (2018) 6940.
10. W. Ying, Y. Li, L. Tang, L. Jin and J. Li, *Electrochem. Commun.*, 11 (2009) 889.
11. C. L. Sun, H. H. Lee, J. M. Yang and C. C. Wu, *Biosens. Bioelectron.*, 26 (2011) 3450.
12. S. A. Kumar, H. W. Cheng and S. M. Chen, *Electroanalysis*, 21 (2010) 2281.

13. W. Wei-Che, C. Han-Wei and T. Yu-Chen, *Chem. Commun.*, 47 (2011) 6458.
14. D. Sun, Z. Qian, T. Feng, X. Wang and J. Gao, *Anal. Methods*, 4 (2012) 3283.
15. C. C. Zhu, Z. Y. Zeng, H. Li, F. Li, C. H. Fan and H. Zhang, *J. Am. Chem. Soc.*, 135 (2013) 5998.
16. S. Su, Z. W. Lu, J. L, Q. Hao, W. Liu, C. C. Zhu, X. Z. Shen, J. Y. Shi and L. H. Wang, *New J. Chem.*, 42 (2018) 6750.
17. X. Chen, Y. J. Park, M. Kang, S. K. Kang, J. Koo, S. M. Shinde, J. Shin, S. Jeon, G. Park and Y. Yan, *Nat. Commun.*, 9 (2018) 1690.
18. H. Sun, J. Chao, X. Zuo, S. Su, X. Liu, L. Yuwen, C. Fan and L. Wang, *RSC Adv.*, 4 (2014) 27625.
19. D. Voiry, R. Fullon, J. Yang, R. Kappera, I. Bozkurt, D. Kaplan, M. J. Lagos, P. E. Batson and G. Gupta, *Nat. Mater.*, 15 (2018) 1003.
20. H. L. Tsai, J. Heising, J. L. Schindler, C. R. Kannewurf and M. G. Kanatzidis, *Chem. Mater.*, 9 (1997) 879.
21. D. A. Voiry, M. Salehi, R. Silva, T. Fujita and M. Chhowalla, *Nano Lett.*, 13 (2013) 6222.
22. J. Z. Ou, A. F. Chrimes, Y. Wang, S. Y. Tang, M. S. Strano and K. Kalantar-Zadeh, *Nano Lett.*, 14 (2014) 857.
23. X. Huang, Z.Y. Zeng, S.Y. Bao, M.F. Wang, X.Y. Qi, Z.X. Fan, H. Zhang, *Nat. Commun.*, 4 (2013) 1444.
24. L. X. Zuo, L. P. Jiang, J. J. Zhu, *Ultrason. Sonochem.*, 35 (2017) 681.
25. W. X. Chen, J. Zhao, J. Y. Lee and Z. L. Liu, *Mater. Chem. Phys.*, 91 (2005) 124.
26. H. G. Wang, P. Chen, F. F. Wen, Y. Zhu, Y Zhang. *Sensor. Actuat. B-Chem*, 220 (2015) 749.
27. Y. Zhang, R. Yuan, Y. Q. Chai, J. F. Wang, H. A. Zhong, *J. Chem. Technol. Biotechnol.*, 87 (2012) 570.
28. J. Chao, X. Y. Han, H. F. Sun, S. Su, L. X. Weng, L. H. Wang, *Sci. China Chem.*, 59 (2016) 332.
29. X. Y. Zheng, X. C. Zhou, X. Ji, R. Y. Lin, W. X. Lin, *Sensor. Actuat. B-Chem*, 178 (2013) 359.
30. L. Q. Lin, J. H. Chen, H. Yao, Y. Z. Chen, Y. J. Zheng, X. H. Lin, *Bioelectrochemistry*, 73 (2008), 73(1):11-17.
31. T. Q. Xu, L. Q. Zhang, J. N. Zheng, Z. Y. Lv, J. Wei, A. J. Wang, J. J. Feng, *Electrochim. Acta*, 115 (2014) 109.
32. C. Q. Wang, J. Du, H. W. Wang, C. E. Zou, F. X. Jiang, P. Yang, Y. K. Du, *Sensor. Actuat. B-Chem.*, 204 (2014) 302.
33. B. B. Yang, H. W. Wang, J. Du, Y. Z. Fu, P. Yang, Y. K. Du, *Colloids Surf., A*, 456 (2014) 146.
34. S. Thiagarajan, S. M. Chen, *Talanta*, 74 (2007) 212.
35. L. Yang, D. Liu, J. S. Huang, T. Y. You, *Sensor. Actuat. B-Chem.*, 193 (2014) 166.
36. B. Kaur, T. Pandiyan, B. Satpati, R. Srivastava, *Colloids Surf. B*, 111 (2013) 97
37. Z. Liu, X. Wang, L. Sun, Z. Y. Yu, *Anal. Methods*, 6 (2014) 9059.

© 2020 The Authors. Published by ESG (www.electrochemsci.org). This article is an open access article distributed under the terms and conditions of the Creative Commons Attribution license (http://creativecommons.org/licenses/by/4.0/).